Synchronously pumped photonic crystal fiber-based optical parametric oscillator

R. T. Murray,[1,*] E. J. R. Kelleher,[1] S. V. Popov,[1] A. Mussot,[2] A. Kudlinski,[2] and J. R. Taylor[1]

[1]*Femtosecond Optics Group, Department of Physics, Imperial College London, Prince Consort Road, London SW7 2BW, UK*

[2]*Laboratoire de Physique des Lasers, Atomes et Molecules (PhLAM), IRCICA, Universite Lille 1, UMR CNRS 8523, 59655 Villeneuve d'Ascq Cedex, France*

**Corresponding author: robert.murray10@imperial.ac.uk*

Received April 25, 2012; revised June 19, 2012; accepted June 23, 2012; posted June 25, 2012 (Doc. ID 167477); published July 25, 2012

We report the development of a compact, tunable synchronously pumped photonic crystal fiber (PCF)-based optical parametric oscillator (FOPO). The oscillator is pumped using a gain-switched laser diode producing 220 ps pulses around 1062 nm, amplified in a ytterbium doped amplifier to peak powers of 3.5 kW. The FOPO produces anti-Stokes pulses at wavelengths between 757 and 773 nm, with durations of 150 ps at average output powers exceeding 290 mW. The output slope efficiency of the device varies with output wavelength from 1.9 to 6.0%.

OCIS codes: 190.4410, 060.5295.

Parametric amplification and wavelength conversion in optical fibers has received considerable attention in recent years in part due to its ability to produce narrow bandwidth laser light in areas that lie outside the emission bands of conventional rare-earth doped fibers. In particular, the pumping of both conventional silica fibers [1,2] and photonic crystal fibers (PCFs) [3–6] in the normal dispersion regime leads to the possibility of very large frequency shifted parametric sidebands from the pump wavelength. Recent parametric conversion sources include using Nd:YAG based pump systems to generate radiation from 0.642 to 3.105 μm, and an all fiber source tunable from 780 to 788 nm based upon a mode-locked Yb-fiber laser [6,7]. Such sources can find applications in both stimulated emission depletion (STED) microscopy and coherent anti-Stokes Raman scattering (CARS) microscopy, where narrow linewidth tunable radiation across the visible regions of the electromagnetic spectrum is required.

By placing the parametric gain fiber into a cavity, such that one or both of the parametrically produced sidebands is resonant, a fiber optic parametric oscillator (FOPO) can be constructed. Oscillators offer obvious advantages over their wavelength converter counterparts such as lower thresholds and higher pump to parametric conversion efficiencies. Compact all fiber parametric oscillators have recently been developed [8], but can suffer from unwanted nonlinear effects in the other fiber components of the system. In this Letter, we present a FOPO device capable of producing clean narrow linewidth anti-Stokes pulses with durations of 150 ps, tunable between 757 and 773 nm, and average powers in excess of 290 mW.

The cavity and associated pump system are shown in Fig. 1. The pump system, Fig. 1(a), consisted of a distributed feedback laser diode (QLD-1064), driven by an external RF pulse generator to produce linearly polarized gain-switched pulses of 220 ps duration between 1060.5 and 1064.0 nm. The diode was driven at a repetition rate of 17.984 MHz, corresponding to half the fundamental round trip frequency. The use of a gain-switched diode, coupled with an adjustable cavity length, rather than a mode-locked pump source, allows the potential for wide tuning of the repetition rate of the FOPO.

The pulses were then amplified in two ytterbium doped fiber amplifiers (YDFAs), before being collimated and passed through a waveplate combination to correct for any nonlinear polarization evolution in the amplifier stages. Through the adjustment of the half wave plate (HWP), the power entering the cavity could be adjusted without affecting the pump pulse duration or spectral linewidth. Finally, the pulses were passed through a bulk optical isolator to prevent any parasitic backreflections from passing from the cavity into the amplifiers. After the amplification stage, the pulses had a maximum peak power of 3.5 kW and exhibited no significant spectral or temporal broadening.

The amplified pulses were then passed into the cavity shown in Fig. 1(b) through a 45° beamsplitter, BS1, with transmission ratios at the pump wavelength of $T_{1060} = 0.992$ and the anti-Stokes signal of $T_{760} = 0.04$. Lens L1 ($f = 3.3$ mm) was used to couple the light into the PCF, with coupling efficiencies of 75%, before being recollimated by an identical lens, L2. The residual pump was then dumped by BS2 ($T_{1060} = 0.032$, $T_{760} = 0.921$), whilst the parametric signal generated in the fiber was allowed to pass. The cavity ends were formed by mirrors

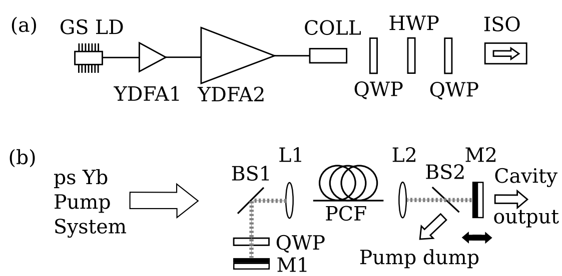

Fig. 1. Schematics of (a) the pump system consisting of a gain-switched laser diode (GS LD), ytterbium doped fiber amplifiers (YDFAs), a collimator (COLL), quarter and half wave plates (QWP/HWP), and an isolator (ISO); (b) the cavity consisting of beamsplitters (BS1/2), focusing lenses (L1/2), photonic crystal fiber (PCF), and mirrors M1/2. Dashed gray line shows path of parametric signal.

0146-9592/12/153156-03$15.00/0

M1, a broadband silver mirror, and M2, the cavity output coupler ($T_{1060} = 0.73$, $T_{760} = 0.12$). M2 was mounted on a translation stage, enabling a tuning of the cavity length by 0.3 m. The quarter wave plate (QWP), was used to correct any polarization evolution in the PCF, to ensure the recirculating signal was in the same polarization state as the pump pulses.

The 2.6 m long PCF used as the nonlinear gain medium was normally dispersive at the pump wavelength, with a zero dispersion wavelength located at 1108 nm. The fiber had a loss of 32 dB/km at 760 nm and 27 dB/km at 1060 nm. The mode field diameter of the fiber was 5.4 μm at 760 nm and 5.5 μm at 1060 nm, and the nonlinear coefficient was 9.2 $W^{-1}\,km^{-1}$ at 1060 nm. A scanning electron microscope image of the fiber can be seen as the inset in Fig. 2. Using this image, the dispersion properties of the fiber were calculated, and used to plot the phasematching curve shown in Fig. 2. By pumping at 1061 nm, parametrically produced frequency sidebands at 761 and 1780 nm were predicted.

By setting the repetition rate of the pump to be half the fundamental of the cavity, and adjusting the cavity length by moving M2, oscillation of the anti-Stokes wavelength was observed. The resulting output spectrum of the cavity when pumped at 1061 nm can be seen in Fig. 3. The linear cavity produces a parametric gain enhancement of more than 45 dB, and when M1 was blocked, no signal was observed.

The inset of Fig. 3 shows the wavelength tuning of the anti-Stokes pump pulses, which was achieved through temperature tuning the gain-switched diode in the range 5–65 °C, corresponding to a pump center wavelength tuning of 1060.5–1064.0 nm. The tuning range of the device could be extended further by means of dispersion tuning, either by adjusting the cavity length or through temperature tuning the PCF [9,10]. The oscillator had an anti-Stokes tuning range of 757–773 nm, and each anti-Stokes spectral line had a 3 dB linewidth no greater than 0.2 nm. The Stokes signal spectrum could not be measured due to restrictions on the range of the optical spectrum analyzer used, but through the use of a high pass optical filter and a pyroelectric power meter, the existence of radiation above 1.75 μm was confirmed.

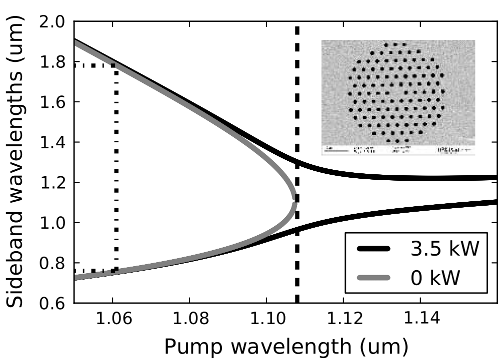

Fig. 2. Phasematching curve for the PCF, calculated from the SEM image shown in the inset, at pump powers of 3.5 and 0 kW. The dotted line shows the zero dispersion wavelength of the PCF, and the dash-dotted line shows the predicted sidebands at a pump wavelength of 1061 nm.

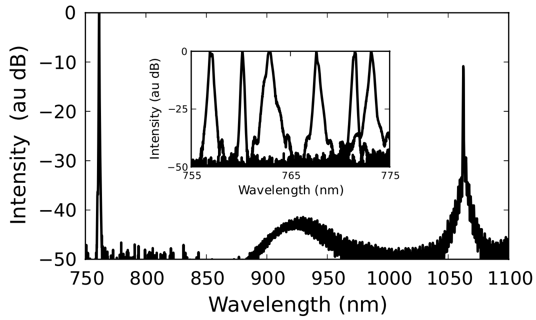

Fig. 3. Output optical spectrum when pumping at 1061 nm. Inset shows the tuning range of the oscillator. Powers are normalized in both the inset and the main figure.

The temporal properties of the pump and associated anti-Stokes pulses were measured using a synchronously scanning streak camera (Hammamatsu OOS-01, resolution of 20 ps), and are shown in Fig. 4. The pump pulses were measured to have a full width half maximum (FWHM) duration of 220 ps and an associated 3 dB linewidth of 0.2 nm. The 762 nm anti-Stokes pulses were measured to have a FWHM duration of 150 ps at an anti-Stokes output power of 153 mW, and an associated 3 dB linewidth of 0.2 nm. The pulse duration was found to decrease with decreasing output power, as a reduction in pump power leads to less of the pump pulse being above the parametric threshold. The anti-Stokes pulses produced from the four-wave mixing process were both temporally shorter and more symmetrical due to the effect of parametric gain shaping.

In order to check the synchronization of the cavity, the mirror M2 was detuned from the cavity harmonic. The output power of the cavity was measured as a function of cavity detuning, and plotted in Fig. 5. The cavity resonates over a distant-equivalent-time of 150 ps, equivalent to the duration of the generated anti-Stokes pulse. Further evidence of synchronization comes from examination of the pump and anti-Stokes pulse shape. The pump possesses a very sharp rising edge, due to the lasing dynamics of the gain-switched laser diode, followed by a slower falling edge. The anti-Stokes pulse, on the other hand, was more symmetric due to the parametric gain shaping. The convolution of two nonidentical pulses, i.e., the pump and anti-Stokes pulse, will create a nonsymmetric profile, as observed in Fig. 5. By tuning back on resonance through adjustment of the repetition rate of the pump source to match the new cavity length,

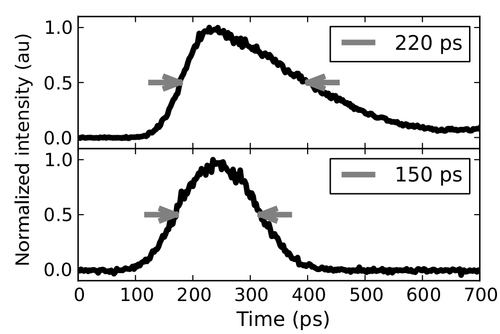

Fig. 4. Temporal measurement of the pump (upper) at 1061 nm and anti-Stokes (lower) pulse at 762 nm.

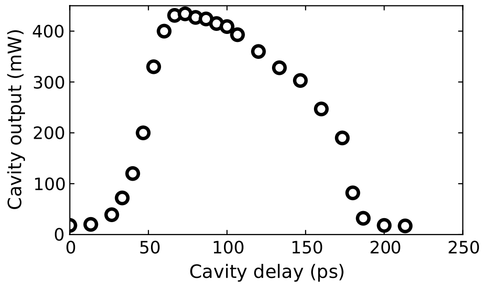

Fig. 5. Total output power of cavity against cavity detuning.

the oscillator was observed to lase, and hence synchronization was verified.

The cavity was found to produce a maximum anti-Stokes output power of 293 mW at a wavelength of 773 nm, corresponding to a pump to anti-Stokes slope conversion efficiency of 6.0%. In Fig. 6, the anti-Stokes output power is plotted as a function of pump power at different wavelengths, along with the associated slope efficiency of the laser. The difference in slope conversion efficiencies is due to the wavelength dependence of the output coupler. It is expected that the overall conversion efficiency was limited by the longitudinal nonuniformity of the PCF, which can significantly alter the phasematching conditions of the fiber from section to section [11]. In addition, linewidth broadening of the pump pulses due to GS operation will restrict the efficiency.

In conclusion, we have demonstrated a compact and tunable synchronously pumped FOPO, emitting 150 ps pulses tunable over the range 757–773 nm with average powers exceeding 290 mW. The novelty of this FOPO resides in the use of a compact gain-switched diode as the seed for the pump source, resulting in more flexible repetition rate and pulse duration tuning. Pumping the oscillator at relatively high repetition rates means the use of additional delay fiber is not required for synchronism. This results in the avoidance of deleterious nonlinear effects due to the peak power of the parametrically produced pulses, such as stimulated Raman scattering or self-phase modulation. By avoiding these effects the pump to parametric conversion efficiency is maximized. Ultimately, the overall pump to anti-Stokes conversion efficiency of the device is limited by fiber inhomogeneities, and the spectral linewidth of the pump source. This source could find applications in both CARS and STED microscopy.

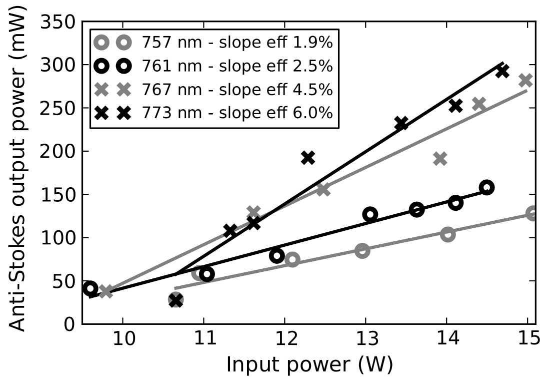

Fig. 6. Pump power at fiber face plotted against power converted into the anti-Stokes sideband, for differing anti-Stokes wavelengths.

EJRK acknowledges funding support from the Engineering and Physical Sciences Research Council (EPSRC), under the EPSRC Doctoral Prize Fellowship.

References

1. G. K. L. Wong, S. G. Murdoch, R. Leonhardt, J. D. Harvey, and V. Marie, Opt. Express **15**, 2947 (2007).
2. Y. Q. Xu and S. G. Murdoch, Opt. Lett. **36**, 4266 (2011).
3. J. D. Harvey, R. Leonhardt, S. Coen, G. K. L. Wong, J. Knight, W. J. Wadsworth, and P. S. Russell, Opt. Lett. **28**, 2225 (2003).
4. D. Nodop, C. Jauregui, D. Schimpf, J. Limpert, and A. Tünnermann, Opt. Lett. **34**, 3499 (2009).
5. L. Lavoute, J. C. Knight, P. Dupriez, and W. J. Wadsworth, Opt. Express **18**, 16193 (2010).
6. A. Herzog, A. Shamir, and A. A. Ishaaya, Opt. Lett. **37**, 82 (2012).
7. M. Baumgartl, M. Chemnitz, C. Jauregui, T. Meyer, B. Dietzek, J. Popp, J. Limpert, and A. Tünnermann, Opt. Express **20**, 4484 (2012).
8. G. Van der Westhuizen and J. Nilsson, in *Conference on Lasers and Electro-Optics* (2011), pp. 1–2.
9. Y. Zhou, K. K. Y. Cheung, Q. Li, S. Yang, P. C. Chui, and K. K. Y. Wong, Opt. Lett. **35**, 2427 (2010).
10. A. Kudlinski, A. Mussot, R. Habert, and T. Sylvestre, IEEE J. Quantum Electron. **47**, 1514 (2011).
11. J. S. Y. Chen, S. G. Murdoch, R. Leonhardt, and J. D. Harvey, Opt. Express **14**, 9491 (2006).